# Fermi Level of Surface States in TiO2 Nanoparticles

**ARTICLE** *in* NANO LETTERS · JUNE 2003

Impact Factor: 13.59 · DOI: 10.1021/nl0342390



**2 AUTHORS:**

Iván Mora-Seró
Universitat Jaume I
**128** PUBLICATIONS **7,649** CITATIONS
SEE PROFILE

Juan Bisquert
Universitat Jaume I
**353** PUBLICATIONS **17,931** CITATIONS
SEE PROFILE

NANO LETTERS

2003
Vol. 3, No. 7
945−949

# Fermi Level of Surface States in $TiO_2$ Nanoparticles

**Ivan Mora-Seró and Juan Bisquert***

*Departament de Ciències Experimentals, Universitat Jaume I, 12080 Castelló, Spain*

*Received April 18, 2003; Revised Manuscript Received May 23, 2003*

## ABSTRACT

**We analyze the nonequilibrium steady-state statistics of electrons in nanoparticulate semiconductors containing a variety of electronic states in relation to applications in dye-sensitized solar cells and photocatalysis. The electrons trapped in surface states do not generally equilibrate to the free electrons' Fermi level, $E_{Fn}$. We show that a distinct Fermi level for surface states, $E_{Fs}$, can be defined consistently with Fermi–Dirac statistics, determining the surface states' occupancy far from equilibrium. The difference $\Delta = E_{Fn} - E_{Fs}$ depends on the rate constants for charge transfer and detrapping and can reach several hundred millielectronvolts. The $E_{Fs}$ becomes a key concept for the analysis of charge transfer and recombination kinetics in nanoparticulate semiconductors.**

**Introduction.** Assemblies of wide band gap semiconductor nanoparticles permeated with an electrolyte (nanoporous electrodes) show promising properties for photovoltaics and catalysis. In dye-sensitized solar cells, electrons generated from visible light at organic molecules adsorbed at the surface are rapidly injected into the conduction band (cb) of the nanoparticles. Alternatively, electron−hole pairs can be generated in the semiconductor particle by UV irradiation. If the hole is rapidly scavenged by species in solution, then long-lived electrons remain in the nanoparticles. In both cases, the effect of the light is to produce a large increase in electron concentration that is exploited in applications (e.g., as a photovoltage). The characterization of the number of photoinjected electrons, their distribution in band gap localized states, and the steps determining electron transfer to species in solution are of fundamental interest and are key points for controlling the operation of devices.

The electrochemical potential, usually denoted as the Fermi level for electrons, is an important concept for analyzing photovoltaic and photoelectrochemical devices.[1,2] In nanoparticulate systems, the injection of photogenerated electrons to the cb causes an upward shift of the free electrons' quasi-Fermi level, $E_{Fn}$ (for brevity, Fermi level), with respect to the dark, equilibrium level that equals the redox potential, $E_{F0} = E_{redox}$. According to the current understanding of nanoporous electrodes, electrons in extended states (with energy $E_c$, concentration $n_c$ and total density $N_c$) communicate with the substrate so that the Fermi level of cb electrons relates to the potential in the outer circuit, $V$, as shown in Figure 1. In addition, semiconductor nanoparticles are known to contain a large number of traps, and the density of trapped charge may largely outnumber that of free-electron charge. A model where traps are considered explicitly was first given by de Jongh and Vanmaekelbergh,[3] and calculations including back reactions through surface states are given in ref 4.

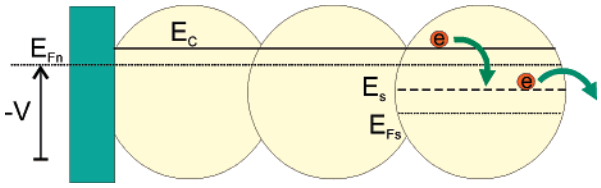


**Figure 1.** Scheme of a semiconductor nanoparticulate electrode sintered over a conducting substrate showing the energy of the transport level ($E_c$) and Fermi level $E_{Fn}$ in relation to the substrate potential $V$, an event of trapping at a surface state ($E_s$) with Fermi level $E_{Fs}$, and subsequent electron transfer from surface states to oxidized species in solution.

We will distinguish two kinds of band gap localized electronic states (as in ref 3): those inside the nanoparticles and those in the surface. The former do not interact directly with the species in solution but only with cb states. Accordingly, internal traps and cb states remain at a common equilibrium even as $E_{Fn}$ rises, implying that the occupancy of these traps $f_t$ at energy $E_t$ is characterized also by $E_{Fn}$ so that the energy level $E = E_{Fn}$ in the band gap separates occupied from unoccupied internal traps. Therefore, we can write

$$n_c = N_c e^{(E_{Fn} - E_c)/k_B T} \quad (1)$$

$$f_t = F(E_t - E_{Fn}) \quad (2)$$

where $k_B T$ is the thermal energy and

* Corresponding author. E-mail: bisquert@uji.es.

10.1021/nl0342390 CCC: $25.00 
**Published on Web 06/20/2003**

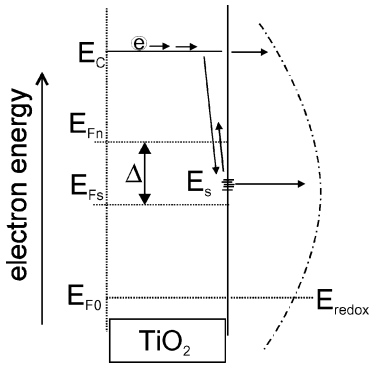


**Figure 2.** Scheme of interfacial electron transfer from a semiconductor nanoparticle to the exponential Gaussian distribution of fluctuating redox species in solution involving direct electron transfer from cb ($E_c$) and also via surface states ($E_s$) mediated by electron capture from the cb. The separate Fermi levels of the cb ($E_{Fn}$) and surface states ($E_{Fs}$) are indicated.

$$F(E_A - E_F) = \frac{1}{1 + e^{(E_A - E_F)/k_B T}} \tag{3}$$

is the Fermi−Dirac distribution function.

Surface states in the band gap often provide the dominant pathway for electron transfer between semiconductor nanoparticles and acceptor species in solution. Although it is often assumed that the occupancy of ss under illumination can also be described by the Fermi level that is common to free electrons and internal traps, this is far from being generally true. When the rate of transfer of electrons from ss to the solution is considerably larger than the rate of detrapping to the cb, the occupancy of those ss is much less than that determined by eq 2.[1] One possible description of this fact is the introduction of a demarcation level[1,5] that separates those ss for which the free electrons' Fermi level does give their occupancy from those for which it does not. However, the usefulness of this concept is limited because it does not indicate the state of occupancy of the latter states as a function of $E_{Fn}$.

In this letter, we show that the occupancy of ss in semiconductor nanoparticles is determined by their own Fermi level, $E_{Fs}$, which is different, in general, from $E_{Fn}$, and the relationship between both will be discussed. This concept of $E_{Fs}$ is similar to the quasi-Fermi levels for trapped holes and electrons in bulk semiconductors,[5] but in our case, it refers to a ss (surface state) that transfers electrons to the solution phase. Furthermore, in nanoporous semiconductors it is important to relate $E_{Fs}$ to $E_{Fn}$ because only $E_{Fn}$ equilibrates directly to the electrochemical potential of electrons in the contact, as indicated in Figure 1. We describe the experimental results on the charge-transfer resistance of UV-irradiated nanoporous $TiO_2$ electrodes in aqueous solution, and we show that the new concept, the surface states' Fermi level, is a key concept for analyzing electron-transfer kinetics in nanoparticulate semiconductors.

**Surface States' Fermi Level.** Let us consider the model for the electron-transfer kinetics in a semiconductor nanoparticle shown in Figure 2. This model involves two classes of electronic states: the cb states and monoenergetic band gap ss at energy $E_s$ with volume concentration $n_s$, total density $N_s$, and fractional occupancy $f_s$ ($n_s = N_s f_s$). We assume that recombination of free electrons occurs by direct electron transfer from cb to oxidized species in solution at a rate $k_{cb}$ and via the ss at a rate $k_s$, and we neglect recombination with holes. The equations of conservation are

$$\frac{\partial n_c}{\partial t} = -\beta n_c[1 - f_s] + \epsilon N_s f_s + G - k_{cb} n_c \tag{4}$$

$$\frac{\partial f_s}{\partial t} = \beta \frac{n_c}{N_s}[1 - f_s] - \epsilon f_s - k_s[f_s - f_{s0}] \tag{5}$$

where $\beta$ and $\epsilon$ are the probabilities of trapping and release, respectively, and $G$ is the rate of electron injection. The probability of trapping is given by

$$\beta = N_s \upsilon \sigma_n \tag{6}$$

Here, $\upsilon$ is the thermal velocity of free electrons, and $\sigma_n$ is the electron capture cross section of the trap (ss). The probability of detrapping is

$$\epsilon = \frac{N_c}{N_s} \beta \exp[-(E_c - E_s)/k_B T] \tag{7}$$

Equation 7 is derived from the condition of microscopic reversibility that implies that the intrinsic transition rates for trapping and detrapping are the same in either direction in thermal dark equilibrium.

As a remark, for nonequilibrium values of the Fermi level, eqs 1 and 2 are consistent with the previous model, eq 5, provided that $k_s = 0$. This proves that internal traps remain at a common equilibrium with the cb in stationary and quasistatic measurements, as indicated in the Introduction. But for a ss with $k_s > 0$, detrapping is not the only mechanism of electron loss from the trap. In the steady state, an electron current determined by $k_s[f_s - f_{s0}]$ is flowing from the cb to the solution through the ss (Figure 1), and $f_s$ is less than in eq 2.

To obtain a statistical expression for $f_s$ in a nonequilibrium steady state, let us assume for simplicity that the occupancy is much larger than the equilibrium value, $f_{s0}$. From eq 5, we obtain

$$f_s = \frac{1}{1 + N_s \dfrac{\epsilon + k_s}{\beta n_c}} \tag{8}$$

Substituting eqs 1 and 7 into eq 8, we get

$$f_s = \frac{1}{1 + \left(1 + \dfrac{k_s}{\epsilon}\right) e^{(E_s - E_{Fn})/k_B T}} \tag{9}$$

This last expression differs from eq 2 only because of the term in $k_s$. Still, we can define the ss Fermi level, $E_{Fs}$,

indicated in Figures 1 and 2 as

$$E_{Fs} = E_{Fn} - \Delta \tag{10}$$

where the Fermi-level difference is given by

$$\Delta = k_B T \ln\left(1 + \frac{k_s}{\epsilon}\right) \tag{11}$$

Then eq 9 can be written as the Fermi−Dirac statistics

$$f_s = F(E_s - E_{Fs}) \tag{12}$$

This result shows that the occupancy of the ss in a nonequilibrium steady state will be completely determined by the position of the ss Fermi level with respect to $E_s$. At $E_{Fs} = E_s$, the ss will be half-occupied, and at $E_{Fs} \gg E_s$, it will be $f_s = 1$. Equation 10 also shows that $E_{Fs}$ always lies below $E_{Fn}$. This is due to the loss of electrons from the ss to the solution. The difference $\Delta$ is determined by the proportion of the rates of transfer of electrons from the ss to the cb (detrapping) and to the oxidized species. If $k_s/\epsilon \ll 1$, then $E_{Fs}$ is approximately equal to $E_{Fn}$; this is the condition described by the demarcation level.[1] Obviously, $\Delta$ becomes much larger than the thermal energy $k_B T$ for $k_s/\epsilon \gg 1$.

**Charge-Transfer Resistance Dependence on the Conduction Band and Surface States' Fermi Levels.** The scheme of the electron exchange process, Figure 2, shows two methods of recombination of the free cb electrons—direct electron transfer from cb to solution and via surface states. Combining eqs 4 and 5 for the steady state and assuming $f_s \gg f_{s0}$, we find that the net rate of recombination of free electrons, $U$, will be

$$U = N_s k_s f_s + k_{cb} n_c \tag{13}$$

The two-step kinetic model involving band gap surface states indicated in eq 13 is well known in the electrochemistry of single-crystal electrodes.[6,7] The electrode potential determines the surface electron concentration through band bending. The current ($I = eU$, where $e$ is the elementary charge) dependence on potential shows two steep rising regions and an intermediate constant range related to the saturation of ss.[7]

The electron-transfer kinetics model for nanoporous electrodes suggested in Figure 2 involves similar mechanisms,[1] but here there are no considerations of band bending. By contrast, as indicated in Figure 1, the electrode potential, $V$, relates simply to the homogeneous Fermi level of free electrons. In photoelectrochemistry, the electrode potential, $V$, is determined by measuring the potential of the conducting substrate with respect to a reference electrode in the solution. In dye-sensitized solar cells, normally the potential of the sensitized electrode is measured with respect to the counterelectrode, which gives the photovoltage as $V = -(E_{Fn} - E_{F0})/e$ (assuming $E_{F0} = E_{redox}$). In any of these cases, a knowledge of $V$ and $\Delta$ completely characterizes the occupancy of both cb and ss and allows a full description of the electron-transfer kinetics to be made with eq 13.

The recombination process can be analyzed using the charge-transfer resistance formalism and impedance spectroscopy technique. Fabregat-Santiago et al.[8,9] found the patterns of charge-transfer resistance as a function of potential in nanostructured $TiO_2$ electrodes in solution. The correlation shows valleys and peaks related to ss saturation and a further increase of the recombination rate through cb, respectively.[8,9] In the following discussion, a detailed physical interpretation of this behavior will be made on the basis of the separate Fermi levels introduced above.

The recombination rate and the charge-transfer differential resistance, $R_F$, are related by

$$R_F = \frac{dV}{dI} = \frac{1}{e}\frac{dV}{dU} \tag{14}$$

Note that the total recombination resistance of the nanoporous film is inversely proportional to its internal area, which in turn is proportional to the film volume. Thus, eq 14 is a specific resistance with units of $\Omega \cdot cm^3$ ($I = eU$ is current per volume). The total resistance is obtained by dividing the specific resistance, $R$, by the electrode volume.

Equation 14 can also be expressed as

$$\frac{1}{R_F} = e\frac{dU}{dn_c}\frac{dn_c}{dV} \tag{15}$$

Combining eqs 1, 13, and 15 and noting from eq 12 that

$$\frac{df_s}{dn_c} = \frac{1}{n_c} f_s(1 - f_s) \tag{16}$$

we obtain expressions for the charge-transfer resistance consisting of two parallel paths shown in Figure 2:

$$R_F^{-1} = R_s^{-1} + R_{cb}^{-1} \tag{17}$$

$$R_s^{-1} = \frac{e}{k_B T} k_s N_s f_s(1 - f_s) n_c \tag{18}$$

$$R_{cb}^{-1} = \frac{e}{k_B T} k_{cb} n_c \tag{19}$$

Equation 18 takes into account the recombination via the surface state, and eq 19, the recombination of the free cb electrons. Because eq 18 contains the product of electron and "hole" probabilities in the ss, $f_s(1 - f_s)$, it follows readily that $R_s$ has a minimum at $E_{Fs} = E_s$.

Finally, according to the Gerischer model, the rate of isoenergetic electron transfer between an energy level, $E$, on the semiconductor surface and fluctuating energy levels in the electrolyte depends on the densities of unoccupied electronic states, $D_{ox}$, of the electrolyte species at energy level $E$,

$$k = 2k_B T k_t D_{ox} \tag{20}$$

$$D_{ox} = \frac{c_{ox}}{\sqrt{4\pi\lambda k_B T}} \exp\left[-\frac{(E - E_{ox})^2}{4\lambda k_B T}\right] \tag{21}$$

where $k_t$ is the volume rate constant for isoenergetic electron transfer, $c_{ox}$ is the concentration of electrolyte oxidized species, $E_{ox}$ is the most probable energy level for oxidized electrolyte species, and $\lambda$ is the reorganization energy $E_{ox} - E_{redox}$. In this sense, transfer rate constants $k_s$ and $k_{cb}$ can be obtained from eqs 20 and 21 for isoenergetic electron transfer at energy levels $E_s$ and $E_c$, respectively.

This model allows us to study the charge-transfer resistance patterns as functions of different parameters. In Figure 3a, the charge-transfer resistance as a function of $E_{Fs}$ is plotted for different concentrations of electrolyte oxidized species $c_{ox}$. The most significant feature of the pattern is the presence of a peak that is a consequence of the two different recombination pathways. If $E_{Fs}$, and consequently $E_{Fn}$, is far from $E_c$, then $n_c$ is not large enough to cause a significant transfer of cb electrons, and the recombination via surface state is the dominant one. When $E_{Fs}$ lies below $E_s$, surface states are not filled, and the occupancy increases as $E_{Fs}$ approaches $E_s$, increasing the recombination current with a consequent diminution of charge-transfer resistance. The minimum of $R_s$ is at $E_{Fs} = E_s$; then when the Fermi trap level overcomes $E_s$, the charge-transfer resistance increases. Physically, when the trap Fermi level overcomes $E_s$, the ss levels are filled, which implies that the current produced by this recombination mechanism saturates. As $E_{Fs}$, and consequently $E_{Fn}$, progresses closer to $E_c$, the recombination via the cb level begins to be significant, and it will be more important than the recombination via ss, governing the behavior of $R_F$, causing a diminution of it, and forming the peak characteristic of the pattern. However, as $c_{ox}$ rises, the rate of recombination increases, which implies a diminution of the charge-transfer resistance.

If we represent the same curves of Figure 3a in a conventional $R_F$ versus potential plot (Figure 3b), then a similar pattern is observed. But now the minimum position is not always at $E_s$; this will occur only when $E_{Fn} \approx E_{Fs}$; otherwise, the minimum will be situated at

$$E_{min} = E_s + \Delta \tag{22}$$

Figure 3c represents the particular case in which $E_c$ and $E_s$ are displaced 5.4 V with respect to the electrolyte oxidized species-level distribution, which remains at the same position, simulating the effect of a change of 9 pH units in an aqueous solution. This displacement causes a $\Delta$ variation as a consequence of the change in the rates of isoenergetic electron transfer, $k_s$ and $k_{cb}$.

**Experimental Results and Discussion.** Electrochemical measurements were made in a standard three-electrode cell using Ag/AgCl (in aqueous 3 M KCl) as a reference electrode and Pt as a counterelectrode. Aqueous electrolytes with 10% ethanol solution were adjusted to pH 2 and 11 with $H_2SO_4$ and KOH, respectively. Ethanol plays the role of a selective scavenger for holes, and it is added to avoid $e^- - h^+$

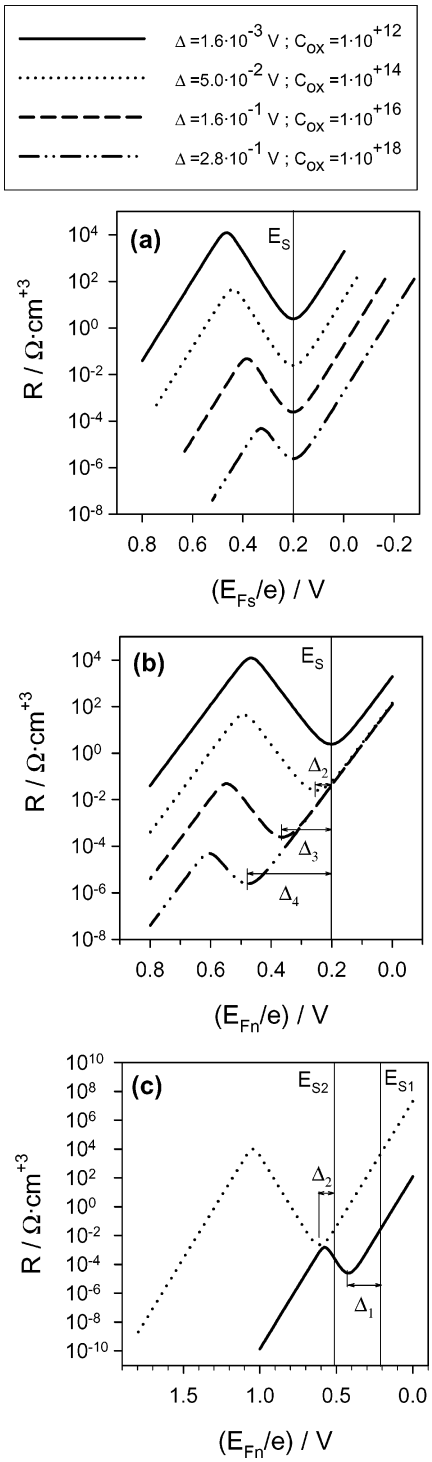


**Figure 3.** (a) Calculated charge-transfer specific resistance vs $E_{Fs}$ and (b) calculated charge-transfer resistance vs $E_{Fn}$ for $E_c = 0.8$ eV, $E_s = 0.2$ eV, $E_{F0} = 0$ eV, $N_c = 1 \times 10^{+21}$ cm$^{-3}$, $N_s = 1 \times 10^{+12}$cm$^{-3}$, $\lambda = 0.2$ eV, $\beta = 1 \times 10^{+8}$ s$^{-1}$, and $k_t = 4 \times 10^{-6}$ cm$^{-3}$ s$^{-1}$ and different concentrations of electrolyte oxidized species $c_{ox}$, as indicated. (c) Calculated charge-transfer resistance for $E_c = 0.8$ eV, $E_s = 0.2$ eV, $\Delta_1 = 0.22$ V (—), $E_c = 1.34$ eV, $E_s = 0.74$ eV, $\Delta_2 = 0.11$ V (···) while the electrolyte oxidized species-level distribution remains at the same position: $E_{F0} = 0$ eV, $c_{ox} = 1 \times 10^{+15}$ cm$^{-3}$, $N_c = 1 \times 10^{+21}$ cm$^{-3}$, $N_s = 1 \times 10^{+12}$ cm$^{-3}$, $\lambda = 0.2$ eV, $\beta = 1 \times 10^{+8}$ s$^{-1}$, and $k_t = 4 \times 10^{-4}$ s$^{-1}$.

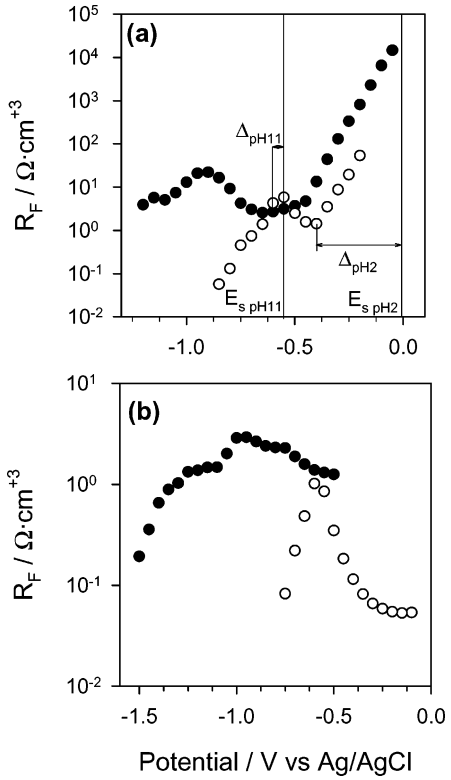


**Figure 4.** Experimental measurements of charge-transfer specific resistance by the impedance method, pH 11 (●), and pH 2 (○). (a) In darkness and (b) under UV illumination.

recombination whereas electrons are transferred predominantly to dissolved oxygen. To study the charge-transfer resistance, impedance measurements were made with an Autolab PGSTAT-30 equipped with a frequency analyzer module. Sintered 12-nm-radius anatase $TiO_2$ colloids deposited on fluoride-doped tin oxide (FTO) were used. Impedance measurements were carried out in the dark and under UV illumination with a 100-W Oriel Xe lamp.

Figure 4 shows the experimental results; Figure 4a in the dark exhibits the characteristic pattern shown in Figure 3. If the occupancy of the ss level is governed by $E_{Fn}$, then the local minimum will determine the trap-level position, and a displacement of 0.54 V (0.06 per pH unit) will be expected. But, as explained before, this will be true only for low $k_s/\epsilon$ ratios, and a lower displacement will occur in the general case as a consequence of the different $\Delta$'s. This has been shown in Figure 3c and is observed in Figure 4a. More specifically, at pH 2 the rate constant for isoenergetic electron transfer, $k$, will be higher for both $k_s$ and $k_{cb}$ than at pH 11. The electrolyte oxidized species-level distribution remains at the same position, and the isoenergetic transfer from $E_c$ and $E_s$ will occur at higher pH to oxidized levels in the Gaussian distribution tail with a lower density of unoccupied electronic states, $D_{ox}$, eq 21. The release probability $\epsilon$ remains unchanged because the relative distance between $E_c$ and $E_s$ does not vary, hence $\Delta_{pH\ 2} > \Delta_{pH\ 11}$. The results in Figure 4 confirm this interpretation. The position of $E_c$ for nanocrystalline anatase $TiO_2$ in aqueous solution has been reported previously;[9] $E_{c\ pH\ 2} = -0.51$ V and $E_{c\ pH\ 11} = -1.05$ V versus Ag/AgCl (3 M KCl). Assuming that the monoenergetic surface state is situated 0.5 V below the lower conduction band edge,[10−12] then $E_{s\ pH\ 2} = -0.01$ V and $E_{s\ pH\ 11} = -0.55$ V versus Ag/AgCl (3 M KCl), and different values of $\Delta$ are obtained for each pH, $\Delta_{pH\ 2} = 0.39$ V and $\Delta_{pH\ 11} = 0.05$ V (Figure 4a). The experimental results also display another feature discussed in Figure 3c. For pH 2, there is a higher recombination and consequently a lower charge-transfer resistance than for pH 11. The peak width also increases for pH 11 because the transfer via the cb level becomes dominant over the recombination via the surface states at a relatively more negative voltage as a consequence of the lower value of $k_{cb}$ for pH 11.

Under illumination (Figure 4b) at positive potentials, the states' population is not determined by the subtrate potential level but by photogeneration−recombination equilibrium in the bulk electrode. As a consequence, the ss occupancy will be constant in this low potential range. A large negative external potential affects the number of electrons, compared with the effect of photogeneration, and the charge-transfer resistance follows the dark pattern showing the peak features at the same potential positions as in the dark.

**Conclusions.** In this letter, we showed that electronic states with different kinetic properties in photon-irradiated nanoparticulate semiconductors do not reach an equilibrium of quasi-Fermi levels at steady-state or quasistatic conditions. We defined the separated Fermi levels that allow us to monitor the occupancy of each kind of state as a function of the electrode potential and to determine the dominant contribution to recombination currents very precisely.

**Acknowledgment.** We are grateful to F. Fabregat-Santiago, P. Salvador, and A. Zaban for useful discussions. This work was supported by the Fundació Caixa-Castelló under project P11B2002-39.

## References

(1) Bisquert, J.; Zaban, A.; Salvador, P. *J. Phys. Chem. B* **2002**, *106*, 8774.
(2) Jakob, M.; Levanon, H.; Kamat, P. V. *Nano Lett.* **2003**, *3*, 353.
(3) de Jongh, P. E.; Vanmaekelbergh, D. *Phys. Rev. Lett.* **1996**, *77*, 3427.
(4) Kambili, A.; Walker, A. B.; Qiu, F. L.; Fisher, A. C.; Savin, A. D.; Peter, L. M. *Physica E* **2002**, *14*, 203.
(5) Simmons, J. G.; Taylor, G. W. *Phys. Rev. B* **1971**, *4*, 502.
(6) Vandermolen, J.; Gomes, W. P.; Cardon, F. *J. Electrochem. Soc.* **1980**, *127*, 324.
(7) Salvador, P.; Gutiérrez, C. *J. Electrochem. Soc.* **1984**, *131*, 326.
(8) Fabregat-Santiago, F.; Garcia-Belmonte, G.; Bisquert, J.; Zaban, A.; Salvador, P. *J. Phys. Chem. B* **2002**, *106*, 334.
(9) Fabregat-Santiago, F.; Mora-Seró, I.; Garcia-Belmonte, G.; Bisquert, J. *J. Phys. Chem. B* **2003**, *107*, 758.
(10) Redmond, G.; Fitzmaurice, D.; Grätzel, M. *J. Phys. Chem.* **1993**, *97*, 6951.
(11) Boschloo, G. K.; Goossens, A. *J. Phys. Chem.* **1996**, *100*, 19489.
(12) Wang, H.; He, J.; Boschloo, G.; Lindström, H.; Hagfeldt, A.; Lindquist, S. *J. Phys. Chem. B* **2001**, *105*, 2529.

NL0342390